



Contents lists available at ScienceDirect

Bioorganic & Medicinal Chemistry Letters

journal homepage: www.elsevier.com/locate/bmcl

Sulfonamide derivatives containing dihydropyrazole moieties selectively and potently inhibit MMP-2/MMP-9: Design, synthesis, inhibitory activity and 3D-QSAR analysis

Xiao-Qiang Yan[†], Zhong-Chang Wang^{†,*}, Zhen Li, Peng-Fei Wang, Han-Yue Qiu, Long-Wang Chen, Xiao-Yuan Lu, Peng-Cheng Lv^{*}, Hai-Liang Zhu^{*}

State Key Laboratory of Pharmaceutical Biotechnology, Nanjing University, Nanjing 210093, People's Republic of China

ARTICLE INFO

Article history:

Received 5 March 2015
Revised 22 July 2015
Accepted 10 August 2015
Available online xxx

Keywords:

Sulfonamide derivatives
Anticancer
MMP-2/MMP-9
Docking
3D-QSAR

ABSTRACT

New series of sulfonamide derivatives containing a dihydropyrazole moieties inhibitors of MMP-2/MMP-9 were discovered using structure-based drug design. Synthesis, antitumor activity, structure–activity relationship and optimization of physicochemical properties were described. In vitro the bioassay results revealed that most target compounds showed potent inhibitory activity in the enzymatic and cellular assays. Among the compounds, compound **3i** exhibited the most potent inhibitory activity with IC₅₀ values of 0.21 μM inhibiting MMP-2 and 1.87 μM inhibiting MMP-9, comparable to the control positive compound **CMT-1** (1.26 μM, 2.52 μM). Docking simulation was performed to position compound **3i** into the MMP-2 active site to determine the probable binding pose. Docking simulation was further performed to position compound **3i** into the MMP-2 active site to determine the probable binding model the 3D-QSAR models were built for reasonable design of MMP-2/MMP-9 inhibitors at present and in future.

© 2015 Elsevier Ltd. All rights reserved.

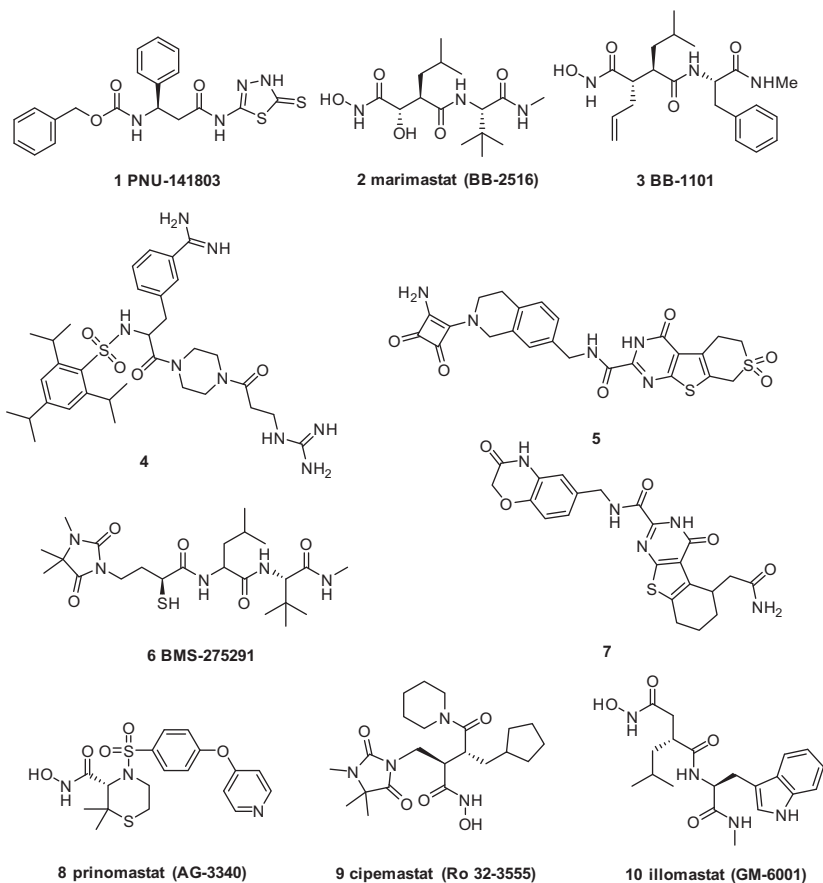
Matrix metalloproteinases (MMPs) are a family of zinc- and calcium-dependent endopeptidases that are capable of degrading and remodeling of connective tissues.^{1,2} Their key roles in physiological tissue remodeling and repair of the extracellular matrix have attracted considerable attention in development of drugs with a potential for therapeutic applications in a variety of diseases including arthritis,^{3,4} tumor growth and metastasis,⁵ periodontal disease,⁶ multiple sclerosis,⁷ and congestive heart failure.^{8,9} These diseases are associated with dysregulated MMP expression and activation. Under normal physiological conditions, activated MMPs are tightly controlled by maintaining a balance between the synthesis of the active forms and their inhibitions by tissue inhibitors of matrix metalloproteinases (TIMPs). The endogenous tissue inhibitors of MMPs could serve as effective

anticancer agents.^{10,11} In addition to other direct TIMP/MMP interactions, the TIMPs also bind to the zinc atom of the active site of the MMPs to block their activity because of containing a Zn²⁺ ion in the catalytic domain.^{12,13} Therefore, inhibiting MMPs is an attractive approach which could treat multitudes of diseases. For example, many inhibitors of MMP-2/MMP-9 have proved to prevent cancer tumor growth.¹⁴ In the joint efforts of a number of laboratories working in the field, many potent and orally active broad-spectrum MMP inhibitors were discovered during the past decade, some of which had reached an advanced clinical trial. Representative examples include **1–8** had been tested against cancers,^{11,15–17} moreover, MMP inhibitors **9** (cipemastat)¹⁸ and **10** (illomastat)¹⁹ were tried in the clinics for inflammation.

* Corresponding authors. Tel./fax: +86 25 83592672.

E-mail address: zhuhl@nju.edu.cn (H.-L. Zhu).

[†] These two authors equally contributed to this paper.



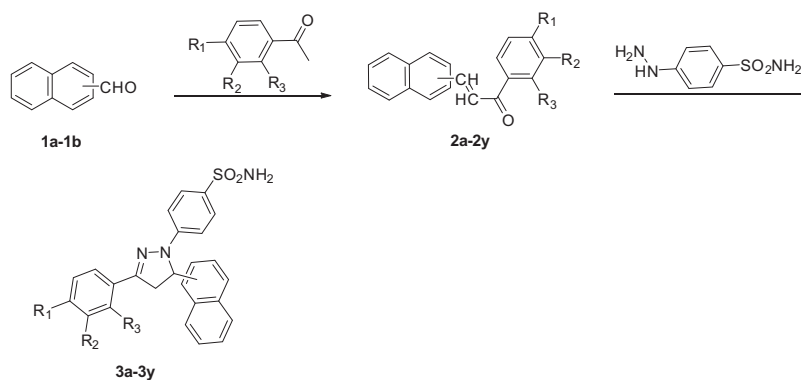
In the last twenty years, scientists in both academia and industry had carried out an industry-wide effort to seek selective MMP inhibitors as innovative medicines.^{20,21} Unfortunately, there had been no clinically useful inhibitor to be demonstrated until now. In general, the major reasons for the failure of these trials were non-specificity, nonselective toxicity and dose-limiting efficacy.²¹ To overcome these present difficulties, we undertook additional efforts to discover the new chelating groups toward the MMP zinc ion,^{22,23} including secondary amine, amide, imine, imidazole, carboxylate, aminocarboxylate, sulfhydryl, hydroxamate, phosphonate and phosphinate moiety and sulfonamides.^{24–29} Sulfonamides had been selected as pharmacological agents due to their biological activities and their potential applications. The application of sulfonamides was widespread due to its anticancer³⁰ and antibacterial.³¹ It recently reported that a series of structurally novel dihydropyrazole derivatives containing the class of primary sulfonamides (RSO₂NH₂), sulfamates (ROSO₂NH₂), and sulfamides (RNHSO₂NH₂) at the *p*-position of the phenyl ring showed substantial antitumor activity, both in vitro and in vivo. Some of these derivatives had been in clinical trials, and there was much optimism that it might contribute to guide novel alternative anticancer drugs, devoid of the side effects of the present available pharmacological agents.^{32,33} Furthermore, special attention had been placed lately on the use of pyrazole for anticancer. Recently, a series of novel pyrazole derivatives were discovered as potent anticancer agents in our group, and some of them had demonstrated potent antitumor activity.^{34,35}

In the preceding work, we have reported the good inhibitory to MMP-2 of a series of benzenesulfonamide benzenesulfonates as a part of our studies on the design and synthesis of MMPs inhibitors.³⁶ Here we extend the earlier work of benzenesulfonamide incorporating benzenesulfonate moieties, and describe the structure-based design and synthesis of novel and potent inhibitors of

MMP-2/MMP-9, utilizing dihydropyrazole and sulfonamide as new structural classes.

The 25 novel sulfonamide derivatives containing dihydropyrazole moieties, as MMP-2/MMP-9 inhibitors (**3a–3y**), were herein synthesized by following the synthetic pathway depicted in Scheme 1. The starting diverse substituted chalcones (**2a–2y**) were synthesized by the substituted acetophenone and equivalent naphthaldehyde in the presence of excess sodium hydroxide, using 40% potassium hydroxide as catalyst in ethanol. Then added acetic acid as acid-binding agent, the cyclization reaction of different chalcones and 4-sulfamoylphenyl hydrazine hydrochloride was in refluxing ethanol for 5–7 h, monitored by thin layer chromatography (TLC). The crude products were purified in good yields, by recrystallization with ethanol, ethyl acetate and acetone (1:1:0.05). All of the target compounds gave satisfactory analytical and spectroscopic data ¹H NMR, EI-MS, which were in accordance with their depicted structures. Furthermore, the crystal structures of compounds **3j**, **3m** and **3s** were determined by single crystal X-ray diffraction analysis in Figure 1 and Table 1.

In the present work, twenty-five of the newly synthesized derivatives (**3a–3y**) were evaluated for their in vitro growth inhibitory activities of four cultured cell lines, which were A549, HeLa, MCF-7 and HepG2 cell lines, comparing with the positive contrast drugs, **Celecoxib** and **Gefitinib**. The IC₅₀ of the compounds against these four human cancer cells were summarized in Table 2. As shown, the results revealed that most of the target compounds exhibited significant anticancer activities, ranging from 1.90 to 50.61 μM. Especially, compound **3i** behaved the most potent anti-tumor activity in A549 cell lines with IC₅₀ of 1.90 μM, compared with the positive control **Gefitinib** (IC₅₀ = 2.86 μM) and **Celecoxib** (IC₅₀ = 2.15 μM). More potent anti-tumor activities for A549 together with virtual screening results indicated that the MMP-2/



Scheme 1. Reagents and conditions: (a) 0.5 equiv 40% potassium hydroxide solution, ethanol, 1.0 equiv different substituted acetophenone, (b) acetic acid, ethanol, 1.2 equiv 4-sulfamoylphenyl hydrazine hydrochloride.

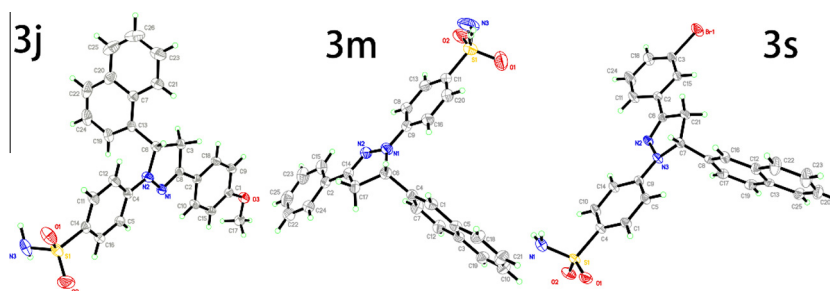


Figure 1. Crystal structure diagrams of compounds **3j**, **3m** and **3s**.

Table 1
Crystal data for compounds **3j**, **3m** and **3s**

Compounds	3j	3m	3s
Empirical formula	C ₂₆ H ₂₃ N ₃ O ₃ S	C ₂₅ H ₂₁ N ₃ O ₂ S	C ₂₅ H ₂₀ BrN ₃ O ₂ S
Formula weight	457.54	427.52	506.41
Temperature (K)	273(2)	273(2)	273(2)
Crystal system	Monoclinic	Monoclinic	Monoclinic
Space group	P21/c (No.14)	P21/c (No.14)	P21/c (No.14)
a (Å)	5.3526(4)	5.5995(6)	9.2897(6)
b (Å)	24.1464(16)	21.282(2)	22.7295(14)
c (Å)	17.5540(16)	17.7413(17)	10.5959(6)
α (°)	90.00	90.00	90.00
β (°)	93.964(2)	98.529(3)	92.995(2)
γ (°)	90.00	90.00	90.00
V (Å ³)	2263.4(3)	2090.9(4)	2234.3(2)
Z	29	27	21
D _{calc} /g cm ⁻³	1.598	1.610	2.419
θ range (°)	2.05–25.14	2.24–25.27	2.12–25.14
F(000)	1102	1026	1533
Reflections collected	21015 (R _{int} = 0.0658)	20029 (R _{int} = 0.1167)	21235 (R _{int} = 0.0585)
Data/restraints/parameters	4043/0/299	3791/0/280	3978/0/280
Absorption coefficient (mm ⁻¹)	0.764	0.770	9.959
R ₁ ; wR ₂ [I > 2σ(I)]	0.0619/0.1495	0.0682/0.1343	0.1252/0.3951
R ₁ ; wR ₂ (all data)	0.1191/0.1769	0.1899/0.1753	0.1660/0.4237
GOF	1.026	1.007	1.679
Larg. peak/hole (e Å ⁻¹)	0.643/–0.388	0.318/–0.285	7.124/–0.697

MMP-9 might be potential targets which these sulfonamide derivatives including dihydropyrazole moieties interacted with.

All the synthesized compounds (**3a–3y**) were tested for MMP-2/MMP-9 inhibitions in comparison to the positive control group **CMT-1** under identical conditions. In this assay, the IC₅₀ values of the target compounds possessing potent inhibitory activity were shown in Table 3. As shown, the results revealed that the majority of the synthesized compounds exhibited significant inhibition activities against MMP-2/MMP-9.

The following structure–activity relationship (SAR) could be observed from data of Table 3, MMP-2/MMP-9 activities of these compounds were tested against the standard clinically inhibitors **CMT-1**. The physiologically dominant matrix metalloproteinases were inhibited by compounds **3a–3y** with IC₅₀ ranging from 0.21 to 23.82 μM for MMP-2, having with IC₅₀ in the range of 1.87–33.75 μM for MMP-9.

Among these given compounds, compound **3i** was the most active with IC₅₀ value of 0.21/1.87 μM, which had stronger

Table 2
In vitro antiproliferation activities (IC₅₀, μM^{a-c}) of target compounds (3a–3y)

Compounds	R ₁	R ₂	R ₃	IC ₅₀ , μM ^{a-c}			
				MCF-7	HeLa	A549	HepG2
<i>α</i> -Naphthyl							
3a	H	H	H	22.62	20.16	12.91	19.08
3b	H	H	CH ₃	10.03	6.37	2.84	5.38
3c	H	H	Cl	23.61	29.07	7.38	10.03
3d	H	CH ₃	H	8.63	9.87	3.14	5.83
3e	H	OCH ₃	H	26.14	30.6	5.82	36.42
3f	H	Br	H	28.83	28.75	8.19	14.92
3g	H	I	H	18.06	26.04	6.83	8.06
3h	CH ₃	H	H	9.89	8.61	7.77	7.04
3i	CH ₃	H	CH ₃	18.06	12.13	1.9	6.99
3j	OCH ₃	H	H	26.37	30.12	6.51	27.76
3k	OCH ₂ CH ₃	H	H	35.05	18.52	3.33	8.66
3l	Cl	H	H	18.02	11.51	2.98	16.45
<i>β</i> -Naphthyl							
3m	H	H	H	21.63	13.04	8.42	17.85
3n	H	H	CH ₃	16.34	15.63	6.84	6.88
3o	H	H	Cl	8.64	16.44	2.16	31.08
3p	H	CH ₃	H	11.08	26.43	7.64	7.68
3q	H	OCH ₃	H	13.56	36.49	8.67	26.04
3r	H	F	H	13.08	21.05	7.83	24.83
3s	H	Br	H	9.15	23.67	10.32	28.98
3t	H	I	H	11.06	32.04	12.04	18.06
3u	CH ₃	H	H	18.17	17.56	6.90	8.32
3v	OCH ₃	H	H	50.61	35.35	9.31	22.32
3w	OCH ₂ CH ₃	H	H	38.23	35.35	17.82	9.17
3x	F	H	H	12.28	26.11	6.95	20.66
3y	Cl	H	H	12.41	19.21	2.76	25.03
Gefitinib	—	—	—	6.71	1.52	2.86	—
Celecoxib	—	—	—	6.88	7.55	2.15	0.76

^a Antiproliferation activity was measured using the MTT assay. Values are the average of six independent experiments run in triplicate. Variation was generally 5–10%.

^b Cancer cells kindly supplied by State Key Laboratory of Pharmaceutical Biotechnology, Nanjing University.

^c Errors were in the range of 5–10% of the reported values, from six different assays.

Table 3
Inhibition activities of compounds (3a–3y) against MMP-2/MMP-9

Compounds	IC ₅₀ , μM ^{a-c}		Compounds	IC ₅₀ , μM ^{a-c}	
	MMP-2	MMP-9		MMP-2	MMP-9
3a	7.92	10.89	3n	11.44	7.91
3b	2.91	5.43	3o	14.83	8.72
3c	8.63	11.97	3p	3.86	5.92
3d	3.24	4.29	3q	2.15	4.68
3e	4.83	6.72	3r	23.82	5.96
3f	11.36	7.97	3s	17.82	13.89
3g	9.43	12.87	3t	15.67	6.91
3h	6.81	15.96	3u	2.81	4.95
3i	0.21	1.87	3v	9.90	18.96
3j	4.27	8.61	3w	14.94	18.31
3k	0.81	3.19	3x	16.84	19.81
3l	2.70	5.47	3y	3.60	5.88
3m	12.63	33.75	CMT-1	1.26	2.52

^a MMP-2/MMP-9 inhibitory activity was measured using the Human Matrix metalloproteinase 2 ELISA kit. Values are the average of six independent experiments run in triplicate. Variation was generally 5–10%.

^b Errors were in the range of 5–10% of the reported values, from six different assays.

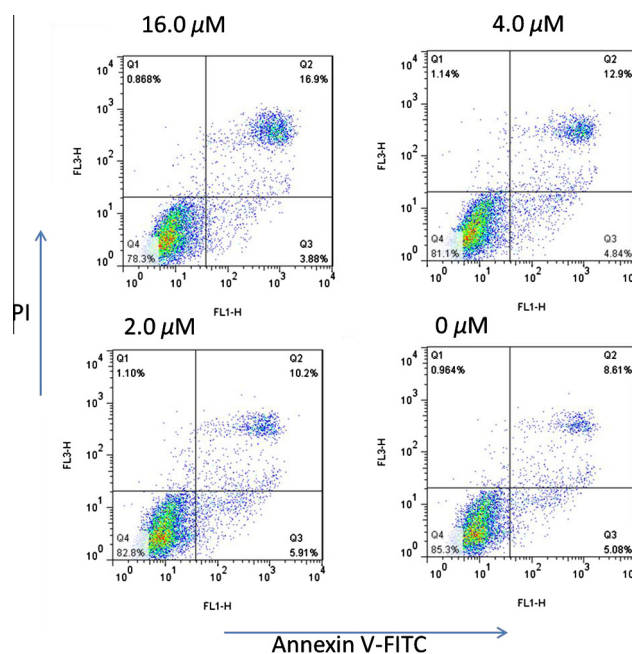
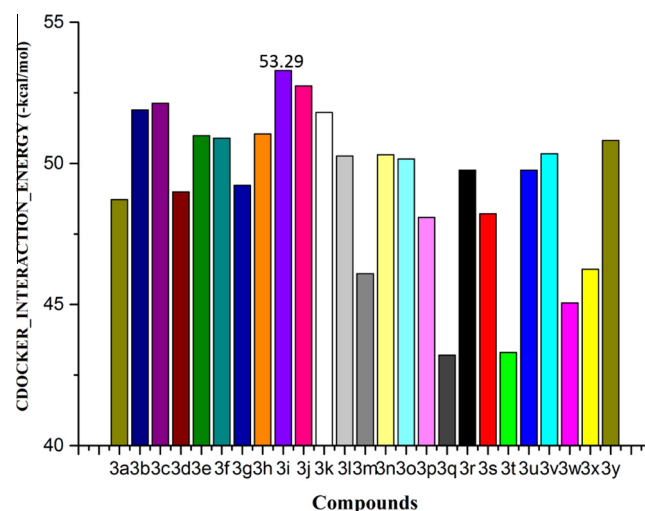
^c Human recombinant enzymes, by the esterase assay (4-nitrophenylacetate as substrate).

MMP-2/MMP-9 inhibition capability than the positive control drug CMT-1 just with IC₅₀ value of 1.26/2.52 μM. Based on the obtained data, we simplified the situations by only treating the single substituent as the single factor to deal with. To begin with, substituents-R², -R³ kept steady, the changes with different

Table 4
The median cytotoxic concentration (CC₅₀) data of all compounds

Compounds	CC ₅₀ ^a (μM)	Compounds	CC ₅₀ ^a (μM)
3a	51.35	3n	51.68
3b	51.23	3o	49.88
3c	53.14	3p	52.41
3d	48.24	3q	49.38
3e	45.32	3r	48.96
3f	42.21	3s	47.04
3g	46.88	3t	55.86
3h	51.26	3u	53.13
3i	52.45	3v	45.40
3j	47.06	3w	53.77
3k	59.50	3x	49.53
3l	49.22	3y	54.76
3m	50.54	Celecoxib	54.38

^a The cytotoxicity of each compound was expressed as the concentration of compound that reduced cell viability to 50% (CC₅₀).

**Figure 2.** Compound 3i induced apoptosis in A549 cells with the density of 0, 2.0, 4.0, 16.0 μM. A549 cells were treated with for 24 h. Values represent the mean ± S. D, n = 3, P < 0.05 versus control. The percentage of cells in each part was indicated.**Figure 3.** The histogram about CDOCKER_INTERACTION_ENERGY (-kcal/mol) of compounds (3a–3y) for MMP-2.

substituents- R^1 for antitumor activity showed the strong electron donor on the para-position were better than electron acceptor or weak electron donor on the same position. For instance, the active gradients for compounds were **3k** ($IC_{50} = 0.81 \mu\text{M}$) > **3l** ($IC_{50} = 2.70 \mu\text{M}$) > **3a** ($IC_{50} = 7.92 \mu\text{M}$), **3w** ($IC_{50} = 14.94 \mu\text{M}$) > **3x** ($IC_{50} = 16.84 \mu\text{M}$). Furthermore, modifying merely substituents- R^2 or $-R^3$, the activity order was shown as follows: **3t** ($IC_{50} = 15.67 \mu\text{M}$) > **3s** ($IC_{50} = 17.82 \mu\text{M}$) > **3r** ($IC_{50} = 23.82 \mu\text{M}$), **3i** ($IC_{50} = 0.21 \mu\text{M}$) > **3h** ($IC_{50} = 6.81 \mu\text{M}$), **3b** ($IC_{50} = 2.91 \mu\text{M}$) > **3c** ($IC_{50} = 8.63 \mu\text{M}$), **3n** ($IC_{50} = 11.44 \mu\text{M}$) > **3m** ($IC_{50} = 12.63 \mu\text{M}$). In view of electronegativity of modified substituents, it was obviously observed that the strong electron donor was very conducive to improve activity correlated with MMP-2.

Besides, it was observed that the IC_{50} values for inhibition of MMP-2 were higher than those observed of MMP-9 with the same variation trend. It was evident that higher concentration of the purified MMP-2 was used than that of MMP-9 in the enzyme

assays. Furthermore, there is also a reasonable correlation coefficient between the two matrix metalloproteinases inhibitory activities. Thus, it is not amazing in view of the high sequence homology of the catalytic domains of these two matrix metalloproteinases.

In comparison, we also found that these compounds with α -naphthyl generally exhibited more potent anticancer activities than those having β -naphthyl. From the above-mentioned analysis, the results of MMP-2/MMP-9 inhibitory activity of the tested compounds correlated with the structure–activity relationships (SAR) of their inhibitory effects on the cell proliferation assay. It could be concluded that the compounds with α -naphthyl were found to be the more favorable for the anticancer activity.

All the target compounds (**3a–3y**) were evaluated for their toxicity against human kidney epithelial cell 293T with the median cytotoxic concentration (CC_{50}) data of tested compounds by the MTT assay. As displayed in Table 4, these compounds were tested at multiple doses to study the viability of macrophage and

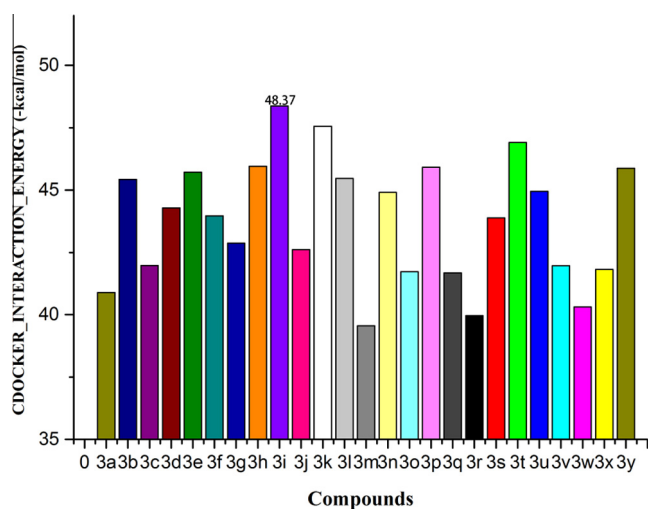


Figure 4. The histogram about CDOCKER_INTERACTION_ENERGY ($-\text{kcal/mol}$) of compounds (**3a–3y**) for MMP-9.

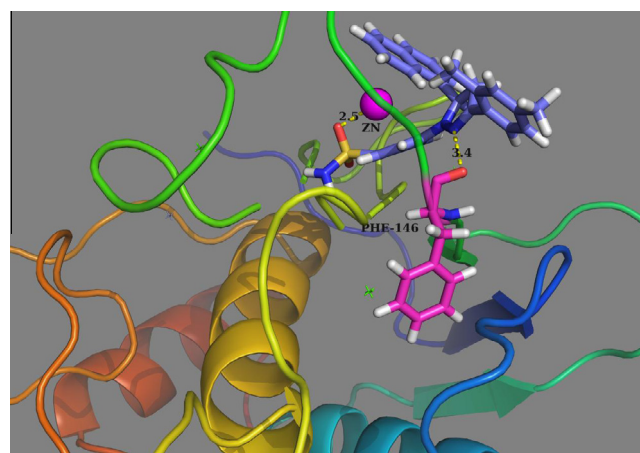


Figure 6. Molecular docking 3D modeling of compound **3i** with the MMP-2 binding site: for clarity, only interacting residues are displayed.

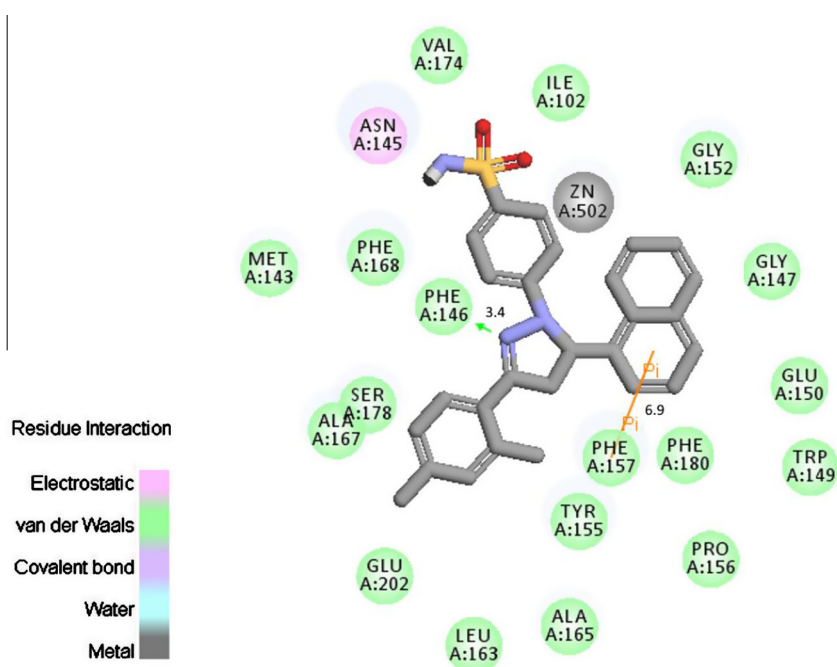


Figure 5. Molecular docking 2D modeling of compound **3i** with MMP-2: for clarity, only interacting residues are displayed.

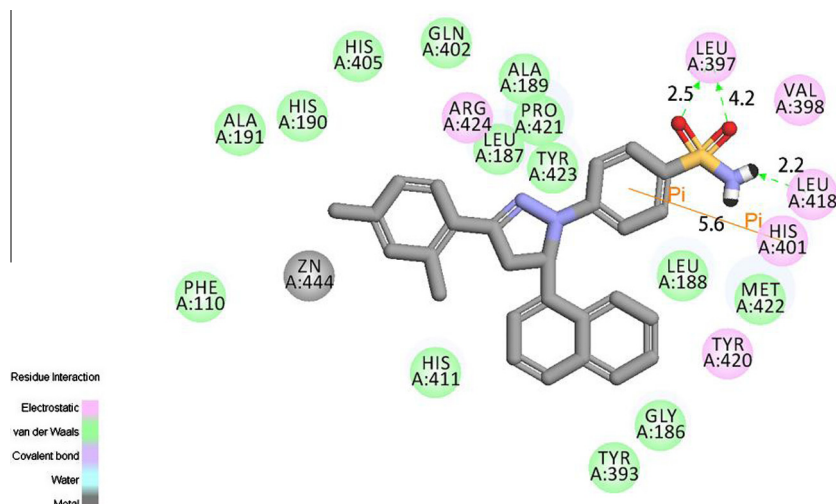


Figure 7. Molecular docking 2D modeling of compound **3i** with MMP-9: for clarity, only interacting residues are displayed.

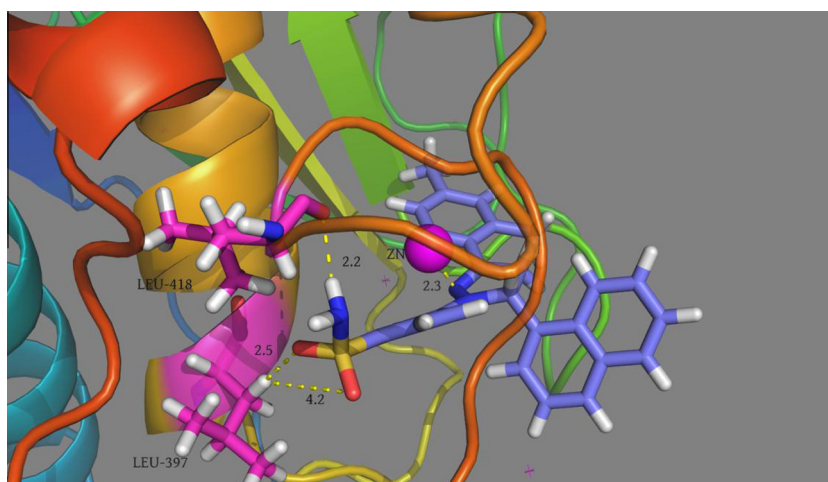


Figure 8. Molecular docking 3D modeling of compound **3i** with the MMP-9 binding site: for clarity, only interacting residues are displayed.

demonstrated almost no cytotoxic activities *in vitro* against human kidney epithelial cell 293T.

To confirm whether the inhibition of cell growth of A549 cell lines was related to cell apoptosis, it was determined to adopt flow cytometry of Annexin V-FITC/PI Apoptosis Detection Kit to induce the A549 cell apoptosis with compound **3i**. The uptake of Annexin V-FITC/PI significantly increased, the uptake of normal cells was significantly decreased in a time-dependent manner. According to the data annotated, the percentage of apoptotic cells was markedly elevated directly and markedly in a manner of dose-dependent. As shown in Figure 2, the percentages of cell apoptosis 20.8%, 17.4%, 16.1%, 13.7% were responding to the concentration of compound **3i** 16.0, 4.0, 2.0, 0 μ M, respectively.

To gain better understanding on the potency of the 25 compounds, we examined the interaction of these compounds with MMP-2/MMP-9 by molecular docking. It was performed on the simulation between the compounds and the ATP binding sites in MMP-2/MMP-9. The protein structures of the MMP-2/MMP-9 were downloaded from the PDB (PDB code: 1QIB and 2OVX), and pre-processed by the DS 3.5 (Discovery Studio 3.5, Accelrys, Co. Ltd.). Hydrogens added to the structure, H-bonds within the protein were optimized, and the protein was minimized to the RMSD of

0.3 Å. A 9.9 Å sphere of water molecules was added around the ligand and a short (3 ps) dynamics run was carried out, followed by several cycles of minimization of Quanta/CHARMM. The entire protein–ligand complex was allowed to move during calculations. The predicted binding interaction energy was used as the criterion for ranking. The estimated interaction energies of other synthesized compounds were ranging from -53.29 to -43.20 , -48.37 to -39.56 kcal/mol, respectively, as displayed in Figures 3 and 4 with histogram. The selected compound of **3i** had a best estimated binding free energy of -53.29 kcal/mol for MMP-2 and -48.37 kcal/mol for MMP-9. The binding mode of compound **3i** interacting with 1QIB protein was exhibited in Figures 5 and 6. The amino acid residues which interacted with the MMP-2 were labeled. In the binding mode, compound **3i** was nicely bound to the ATP binding site including one hydrogen bond with the backbone NH of **Phe146** (angle O–H...N = 148.52° , distance = 3.4 Å) and a π -cation interaction between the backbone **Phe157** (distance = 6.9 Å). Besides, one coordinate bond was formed between zinc cation and oxygen atoms (distance = 2.5 Å), which increased the binding affinity dramatically in theory, as displayed in Figure 6. There was the binding mode of compound **3i** interacting with 2OVX protein in Figures 7 and 8. As shown, three amino acids,

Table 5

The Experimental and predicted inhibitory activity of compounds (**3a–3y**) by 3D-QSAR models based upon active conformation achieved by molecular docking

Compounds ^a	MMP-2		Residual error
	Actual pIC ₅₀	Predicted pIC ₅₀	
3a	5.10	5.09	0.01
3b	5.54	5.54	0.00
3c	5.07	5.04	0.03
3d	5.49	5.54	-0.05
3e	5.32	5.08	0.24
3f	4.95	4.88	0.07
3g	5.03	5.00	0.03
3h	5.17	5.28	-0.11
3i	6.68	6.71	-0.03
3j	5.38	5.39	-0.01
3k	6.10	5.83	0.27
3l	5.57	5.50	0.07
3m	4.90	5.08	-0.18
3n	4.94	4.96	-0.02
3o	4.83	5.27	-0.44
3q	5.68	5.67	0.01
3p	5.42	5.46	-0.04
3r	4.62	4.65	-0.03
3s	4.75	4.72	0.03
3t	4.81	4.91	-0.10
3u	5.55	5.54	0.01
3v	5.00	4.97	0.03
3w	4.83	4.81	0.02
3x	4.77	4.87	-0.10
3y	5.44	5.38	0.06

^a The underlined for the test set, and the rest for training.

Leu397, **Leu418** and **His401**, were of significance in the binding of ligand with enzyme of 2OVX. Moreover, the **Leu397** formed two hydrogen bonds with **3i** (angle O··H–N = 132.7°, distance = 2.5 Å, angle O··H–N = 92.5°, distance = 4.2 Å). Furthermore, compound **3i** was also bonded with **Leu418** by a hydrogen (angle O··H–N = 112.4°, distance = 2.2 Å) and **His401** by a Pi bond. As exhibited in **Figure 8**, there was also a ATP binding site of a coordinate bond between zinc cation and nitrogen atoms (distance = 2.3 Å). According to the above, these molecular docking results along with the biological assay data suggested that compound **3i** might be a potential inhibitor of the MMP-2.

In order to obtain the systematic SAR profile on sulfonamide derivatives containing dihydropyrazole moieties (**3a–3y**) as antitumor agents and explore the more powerful and selective inhibitors of MMP-2, 3D-QSAR models³⁷ were built according to the compounds synthesized and their corresponding capability. By this effort, we intended to explain the mechanism of the SAR and cast a light on the discovery of more potent novel antagonist of MMP-2. This model was performed by built-in QSAR software of DS 3.5 with all the molecular converted to the active conformation and corresponding pIC₅₀ (μM) values, which were converted from the obtained IC₅₀ (μM) values of MMP-2 inhibition. These compounds were divided into a test set composing 20 agents and a relative training set including 5 agents by the random, which had been presented in **Table 5**.

By default, the alignment conformation of each molecule possessed the lowest CDOCKER_INTERACTION_ENERGY among all of the docked poses. The critical regions (steric or electrostatic) affecting the binding affinity was gained by this 3D-QSAR model. Exerting CHARMM force filed and PLS regression, the model was set up with the correlation coefficient R^2 is 0.922, and the leave-one-out cross validation coefficient q^2 is 0.469. Besides, the RMS error, the mean absolute error, R^2_{pred} and F are 0.249, 0.214, 0.834 and 101.916, respectively. These details indicated that this

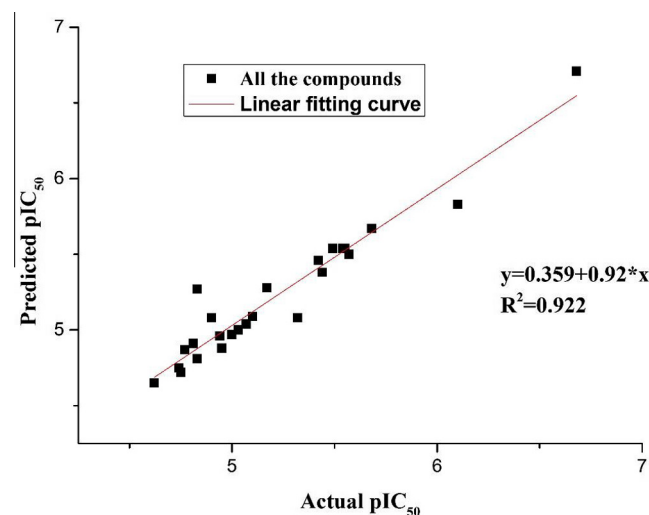


Figure 9. Comparing the predicted pIC₅₀ value about MMP-2 inhibitory activities with that of the experiment by linear fitting curve.

model possessed pretty good predicting capability. The relationship between observed and predicted values had been shown graphically in **Figure 9**.

Also the molecules aligned with the iso-surfaces of the 3D-QSAR model coefficients on electrostatic potential grids **Figure 10(a)** and Van der Waals grids **Figure 10(b)** were listed. Electrostatic map were depicted below to display the favorable (in blue) or unfavorable (in red) electrostatic field region in a contour plot, while the energy grids corresponding to the favorable (in green) or unfavorable (in yellow) steric effects were also marked out. For compounds based on the 3D-QSAR model, possessing strong Van der Waals attraction in the green areas and a polar group in the blue electrostatic potential areas mean achieving potent bioactivity. This model was accordant with the actual situation for compounds. Accordingly, this promising model would provide a guideline to design and optimize more effective tubulin inhibitors and pave the way for us in the further study.

In summary, novel series of sulfonamide derivatives including dihydropyrazole moieties (**3a–3y**) had been evaluated for anticancer activities against MCF-7, HeLa, A549, HepG2 cell lines and MMP-2/MMP-9 inhibitory activities. These compounds showed a very interesting profile for the inhibition of MMP-2/MMP-9, which mostly exhibited potent anticancer and MMP-2/MMP-9 inhibitory activities, with IC₅₀ ranging from 1.90 to 50.61 μM, 0.21 to 23.82 μM and 1.87 to 33.75 μM, respectively. Moreover, most of them showed almost no toxicity towards 293T. Among them, compound **3i** exhibited the most potent MMP-2/MMP-9 inhibition activities (IC_{50,MMP-2} = 0.21 μM, IC_{50,MMP-9} = 1.87 μM). Besides, the probable binding models and poses were obtained by docking simulation. Analysing the binding model of compounds **3i** with MMP-2, there were a hydrogen bond, a π-cation interaction with the protein residues and a coordinate bonds with Zinc Ion in the ATP binding site, which might play a crucial role in its MMP-2 inhibition and antiproliferative activities. Furthermore, three hydrogen bonds, a Pi bond and a coordinate bonds with Zinc Ion formed the major acting force in the binding model of compounds **3i** with MMP-9. Last but not least, 3D-QSAR models were built with previous activity data and binding conformations to begin our work in this paper as well as to provide a reliable tool for reasonable design and synthesis of potent MMP-2 inhibitors.

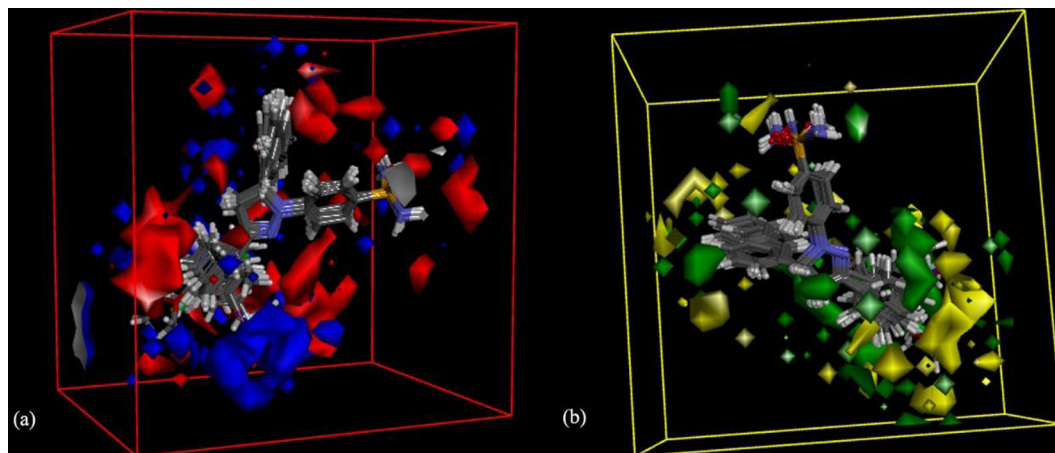


Figure 10. (a) Isosurface of the 3D-QSAR model coefficients on electrostatic potential grids. Blue represents positive coefficients; red represents negative coefficients. (b) Isosurface of the 3D-QSAR model coefficients on Van der Waals grids. Green represents positive coefficients; yellow represents negative coefficients

Acknowledgments

The work was financed by a Grant (No. J1103512) from National Natural Science Foundation of China and the Research Innovation Program for College Graduates of Jiangsu Province in 2014 (No. SJZZ_0015).

Supplementary data

Supplementary data associated with this article can be found, in the online version, at <http://dx.doi.org/10.1016/j.bmcl.2015.08.026>.

References and notes

- Schröder, J.; Henke, A.; Wenzel, H.; Brandstetter, H.; Stammler, H. G.; Stammler, A.; Pfeiffer, W. D.; Tschesche, H. *J. Med. Chem.* **2001**, *44*, 3231.
- Rizzo, R. C.; Toba, S.; Kuntz, I. D. *J. Med. Chem.* **2004**, *47*, 3065.
- Firestein, G. S.; Paine, M. M.; Littman, B. H. *Arthritis Rheum.* **1991**, *1094*, 34.
- Walakovits, L. A.; Moore, V. L.; Bhardwaj, N.; Gallick, G. S.; Lark, M. W. *Arthritis Rheum.* **1992**, *35*, 35.
- Pyke, C.; Ralfkiaer, E.; Huhtala, P.; Hurskainen, T.; Danø, K.; Tryggvason, K. *Cancer Res.* **1992**, *52*, 1336.
- Overall, C. M.; Wiebkin, O. W.; Thonard, J. C. *J. Periodontol Res.* **1987**, *22*, 81.
- Gijbels, K.; Galardy, R. E.; Steinman, L. J. *Clin. Invest.* **1994**, *94*, 2177.
- Coker, M. L.; Thomas, C. V.; Clair, M. J.; Hendrick, J. W.; Krombach, R. S.; Galis, Z. S.; Spinale, F. G. *Am. J. Physiol. Heart Circ. Physiol.* **1998**, *274*, 1516.
- Spinale, F. G.; Coker, M. L.; Krombach, S. R.; Mukherjee, R.; Hallak, H.; Houck, W. V.; Clair, M. J.; Kribbs, S. B.; Johnson, L. L.; Peterson, J. T.; Zile, M. R. *Circ. Res.* **1999**, *85*, 364.
- Overall, C. M.; Lopez-Otin, C. *Nat. Rev. Cancer* **2002**, *2*, 657.
- Pochetti, G.; Montanari, R.; Gege, C.; Chevrier, C.; Taveras, A. G.; Mazza, F. *J. Med. Chem.* **2009**, *1040*, 52.
- Hugenberg, V.; Riemann, B.; Hermann, S.; Schober, O.; Schäfers, M.; Szardenings, K.; Lebedev, A.; Gangadharmath, U.; Kolb, H.; Walsh, J.; Zhang, W.; Kopka, K.; Wagner, S. *J. Med. Chem.* **2013**, *56*, 6858.
- Selivanova, S. V.; Stellfeld, T.; Heinrich, T. K.; Müller, A.; Krämer, S. D.; Schubiger, P. A.; Schibli, R.; Ametamey, S. M.; Vos, B.; Meding, J.; Bauser, M.; Hütter, J.; Dinkelborg, L. M. *J. Med. Chem.* **2013**, *56*, 4912.
- Rothenberg, M. L.; Nelson, A. R.; Hande, K. R. *Oncologist* **1998**, *3*, 271.
- Rosenbaum, E.; Zahurak, M.; Sinibaldi, V.; Carducci, M. A.; Pili, R.; Laufer, M.; DeWeese, T. L.; Eisenberger, M. A. *Clin. Cancer Res.* **2005**, *11*, 4437.
- Bissett, D.; O'Byrne, K. J.; von Pawel, J.; Gatzemeier, U.; Price, A.; Nicolson, M.; Mercier, R.; Mazabel, E.; Penning, C.; Zhang, M. H.; Collier, M. A.; Shepherd, F. A. *J. Clin. Oncol.* **2005**, *23*, 842.
- Steinmetzer, T.; Schweinitz, A.; Stürzebecher, A.; Dönnecke, D.; Uhland, K.; Schuster, O.; Steinmetzer, P.; Müller, F.; Friedrich, R.; Than, M. E.; Bode, W.; Stürzebecher, J. *J. Med. Chem.* **2006**, *49*, 4116.
- Hemmings, F. J.; Farhan, M.; Rowland, J.; Banken, L.; Jain, R. *Rheumatology* **2001**, *40*, 537.
- Paul Beckett, R. *Expert Opin. Ther. Pat.* **1996**, *6*, 1305.
- Skiles, J. W.; Gonnella, N. C.; Jeng, A. Y. *Curr. Med. Chem.* **2004**, *11*, 2911.
- Li, J. J.; Nahra, J.; Johnson, A. R.; Bunker, A.; O'Brien, P.; Yue, W. S.; Ortwine, D. F.; Man, C. F.; Baragi, V.; Kilgore, K.; Dyer, R. D.; Han, H. K. *J. Med. Chem.* **2008**, *51*, 835.
- Pirard, B. *Drug Discovery Today* **2007**, *12*, 640.
- Georgiadis, D.; Yiotakis, A. *Bioorg. Med. Chem.* **2008**, *16*, 8781.
- Hidalgo, M.; Eckhardt, S. G. *J. Natl Cancer Inst.* **2001**, *93*, 178.
- Burdette, S. C.; Frederickson, C. J.; Bu, W.; Lippard, S. J. *J. Am. Chem. Soc.* **2003**, *125*, 1778.
- Larionov, S. V.; Savel'eva, Z. A.; Klevtsova, R. F.; Uskov, E. M.; Glinskaya, L. A.; Popov, S. A.; Tkachev, A. V. *Russ. J. Coord. Chem.* **2011**, *37*, 1.
- Zhao, N.; Chen, L.; Ren, W.; Song, H.; Zi, G. *J. Organomet. Chem.* **2012**, *712*, 29.
- Katayev, E. A.; Schmid, M. B. *Dalton Trans.* **2011**, *40*, 2778.
- Brzozowski, Z.; Sławiński, J.; Vullo, D.; Supuran, C. T. *Eur. J. Med. Chem.* **2012**, *56*, 282.
- Supuran, C. T.; Scozzafava, A. *Expert Opin. Ther. Pat.* **2000**, *10*, 575.
- Drews, J. *Science* **2000**, *287*, 1960.
- Winum, J. Y.; Scozzafava, A.; Montero, J. L.; Supuran, C. T. *Anti-Cancer Agent Med.* **2009**, *9*, 693.
- El-Sayed, N. S.; El-Bendary, E. R.; El-Ashry, S. M.; El-Kerdawy, M. M. *Eur. J. Med. Chem.* **2011**, *46*, 3714.
- Ly, P. C.; Li, H. Q.; Sun, J.; Zhou, Y.; Zhu, H. L. *Bioorg. Med. Chem.* **2010**, *18*, 4606.
- Qiu, K. M.; Wang, H. H.; Wang, L. M.; Luo, Y.; Yang, X. H.; Wang, X. M.; Zhu, H. L. *Bioorg. Med. Chem.* **2012**, *20*, 2010.
- Qiu, H. Y.; Wang, Z. C.; Wang, P. F.; Yan, X. Q.; Wang, X. M.; Yang, Y. H.; Zhu, H. L. *RSC Adv.* **2014**, *4*, 39214.
- Egan, W. J.; Merz, K. M.; Baldwin, J. J. *J. Med. Chem.* **2000**, *43*, 3867.